Available online at www.sciencedirect.com
SCIENCE DIRECT
Science Press
Trans. Nonferrous Met. Soc. China 18(2008) 59−65
Transactions of Nonferrous Metals Society of China
www.csu.edu.cn/ysxb/

Microscopic phase-field simulation of atomic site occupation in ordering process of $NiAl_9Fe_6$ alloy

LIANG Min-jie(梁敏洁), CHEN Zheng(陈 铮), ZHANG Ji-xiang(张济祥), WANG Yong-xin(王永欣)
School of Materials Science and Engineering, Northwestern Polytechnical University, Xi'an710072, China

Received 13 April 2007; accepted 26 June 2007

Abstract: The process of γ(fcc)→γ(fcc)+$\gamma'(L1_2)$ phase transformation was simulated by using microscopic phase-field method for the low supersaturation $NiAl_9Fe_6$ alloy. It is found that in the γ' phase, the ordering degree of Al atoms is obviously higher than that of Fe atoms, and the ordering of Al atoms precedes their clustering, while the case of Fe atoms is opposite. The α site is mainly occupied by Ni atoms, while the β site is occupied in common by Al, Fe and Ni atoms. At order-disorder interphase boundary, the ordering degree of Al atoms is higher than that of Fe atoms, and at the β site, the Fe atomic site occupation probabilities vary from high to low during ordering; the Al atomic site occupation probabilities are similar to those of Fe atoms, but their values are much higher than those of Fe atoms; Ni atoms are opposite to both of them. Meanwhile, during the ordering transformation, γ' phase is always a complex Ni_3(AlFeNi) single-phase, and it is precipitated by the non-classical nucleation and growth style. Finally, in the alloy system, the volume of γ' ordered phase is less than that of γ phase, and the volume ratio of order to disorder is about 77%.

Key words: microscopic phase-field; Ni-Al-Fe alloy; $\gamma'(L1_2)$; site occupation; ordering

1 Introduction

The Ni_3Al (γ'-phase) intermetallics has a long-range ordered superstructure of the $L1_2$ type, and its special characteristic that yield stress abnormally increases with temperature rising attracts the people's attentions[1−3]. However, the single crystal and polycrystal Ni_3Al has a lower yield stress, which should be strengthened by the alloying method in order to eliminate the intercrystalline brittleness. Meanwhile, the site occupation of the corner (β site) and the face-center (α site) of the $L1_2$ superstructure is very different due to the distinction of added elements, so the strengthening effects are greatly influenced. In Ni_3Al, the solute Fe element can occupy both Ni and Al sites so that formed γ' phase is relatively complex[4−7]. There are some researches on the γ' phase of Ni-Al-Fe alloy, for instance, KOZUBSKI and SOLTYS[8] studied the long-range ordering kinetics evolution of quasi-binary $Ni_{75}Al_{25-x}Fe_x$ system by means of the experiments; CAHN[2] investigated the order-disorder transformation in Ni_3Al-Fe alloy by the experiments; ALMAZOUZI et al[9] and ANNIE et al[10] used the atom-probe, etc, experimental methods to study the substitution behavior of Fe in Ni_3Al; JIANG and GLEESON[11] studied the site occupation behavior of Fe in Ni_3Al as a function of both alloy composition and temperature by the first-principles calculations. However, the works above are mostly focused on experiments, and the simulations about order-disorder transformation are relatively few for Ni-Al-Fe alloy. The discrepancy about atomic sites occupation behavior of the γ' ordered phase still exists in the experimental and the theoretic studies. Meanwhile, in these studies such as the concrete precipitation mechanism of γ' phase and the evolution rules of atomic site occupation with the time changing for the low supersaturation Ni-Al-Fe alloy have not been reported.

In view of the applied and theoretic significance, the purpose of present study is to simulate the γ(fcc)→γ(fcc)+$\gamma'(L1_2)$ phase transformation of low supersaturation $NiAl_9Fe_6$ alloy aged at 873 K, based on the microscopic phase-field model. In this work, the authors not only presented the concrete precipitation mechanism of γ' phase but also further developed this model to study the rules of the atomic site occupation during ordering transformation at γ' phase and order-disorder interphase boundary. The obtained micro-evolution by simulation

Foundation item: Project(50671084) supported by the National Natural Science Foundation of China; Project(Z200714) supported by Graduate Starting Seed Fund of Northwestern Polythechnical University, China
Corresponding author: LIANG Min-jie; Tel: +86-29-88474095; Fax: +86-29-88486023; E-mail: lmj2005686@sina.com

has a certain theoretic significance to further study and improve the mechanical property of the Ni-Al-Fe alloy.

2 Microscopic phase-field kinetic model

Microscopic phase-field kinetic model, based on the microscopic crystal lattice diffusion theory proposed by KHACHATURYAN[12], is the development of Ginzburg-Landau continuous phase-field model used to simulate the phase separation phenomenon. Composition and long-range order (l.r.o.) parameter could be contacted by the non-equilibrium free energy function in alloy. In recent years microscopic phase-field kinetic model has been developed to the ternary alloy system by CHEN et al[13−14]. In this simulation, $P_A(\boldsymbol{r}, t)$, $P_B(\boldsymbol{r}, t)$, $P_C(\boldsymbol{r}, t)$ represent the probabilities of locating an A, B or C atom at a given lattice site $\boldsymbol{r}$ and a given time t, respectively. Since the probability sum of three atoms is 1, only two equations are independent at each lattice site. Microscopic diffusion equation for the ternary system is written as

$$\begin{cases}\dfrac{\mathrm{d}P_A(\boldsymbol{r},t)}{\mathrm{d}t}=\dfrac{1}{k_BT}\cdot\\ \quad\displaystyle\sum_{\boldsymbol{r}'}\left[L_{AA}(\boldsymbol{r}-\boldsymbol{r}')\frac{\partial F}{\partial P_A(\boldsymbol{r}',t)}+L_{AB}(\boldsymbol{r}-\boldsymbol{r}')\frac{\partial F}{\partial P_B(\boldsymbol{r}',t)}\right]\\ \dfrac{\mathrm{d}P_B(\boldsymbol{r},t)}{\mathrm{d}t}=\dfrac{1}{k_BT}\cdot\\ \quad\displaystyle\sum_{\boldsymbol{r}'}\left[L_{BA}(\boldsymbol{r}-\boldsymbol{r}')\frac{\partial F}{\partial P_A(\boldsymbol{r}',t)}+L_{BB}(\boldsymbol{r}-\boldsymbol{r}')\frac{\partial F}{\partial P_B(\boldsymbol{r}',t)}\right]\end{cases} \tag{1}$$

where $L_{\alpha\beta}(\boldsymbol{r}-\boldsymbol{r}')$ is the constant that is related to the exchange probability of a pair of atoms, α and β, at lattice site $\boldsymbol{r}$ and $\boldsymbol{r}'$ per unit time, α and β are A, B or C; F is the total free energy of the system.

Eqn.(1) could be turned into a random equation by adding a random noise item to simulate the thermal fluctuation, and then the microscopic Langevin equation is obtained by Fourier transform in the reciprocal space:

$$\begin{cases}\dfrac{\mathrm{d}\tilde{P}_A(\boldsymbol{k},t)}{\mathrm{d}t}=\dfrac{1}{k_BT}\displaystyle\sum_{\boldsymbol{r}'}\left[\tilde{L}_{AA}(\boldsymbol{k})\left(\frac{\partial F}{\partial P_A(\boldsymbol{r}',t)}\right)_{\boldsymbol{k}}+\right.\\ \qquad\left.\tilde{L}_{AB}(\boldsymbol{k})\left(\frac{\partial F}{\partial P_B(\boldsymbol{r}',t)}\right)_{\boldsymbol{k}}\right]\xi(\boldsymbol{k},t)\\ \dfrac{\mathrm{d}\tilde{P}_B(\boldsymbol{k},t)}{\mathrm{d}t}=\dfrac{1}{k_BT}\displaystyle\sum_{\boldsymbol{r}'}\left[\tilde{L}_{BA}(\boldsymbol{k})\left(\frac{\partial F}{\partial P_A(\boldsymbol{r}',t)}\right)_{\boldsymbol{k}}+\right.\\ \qquad\left.\tilde{L}_{BB}(\boldsymbol{k})\left(\frac{\partial F}{\partial P_B(\boldsymbol{r}',t)}\right)_{\boldsymbol{k}}\right]+\xi(\boldsymbol{k},t)\end{cases} \tag{2}$$

where $\boldsymbol{k}$ is the reciprocal lattice vector within the first Brillouin zone, $\tilde{P}_A(\boldsymbol{k}, t)$, $\tilde{P}_B(\boldsymbol{k}, t)$, $\tilde{L}_{AA}(\boldsymbol{k})$, $\tilde{L}_{AB}(\boldsymbol{k})$, $\tilde{L}_{BA}(\boldsymbol{k})$, $\tilde{L}_{BB}(\boldsymbol{k})$, and $\zeta(\boldsymbol{k}, t)$ are Fourier transform of corresponding functions in the real space. In the mean-field approximation, F are given by

$$\begin{aligned}F=&-\frac{1}{2}\sum_{\boldsymbol{r}}\sum_{\boldsymbol{r}'}[V_{AB}(\boldsymbol{r}-\boldsymbol{r}')P_A(\boldsymbol{r})P_B(\boldsymbol{r}')+V_{BC}(\boldsymbol{r}-\boldsymbol{r}')P_B(\boldsymbol{r})\cdot\\ &P_C(\boldsymbol{r}')+V_{AC}(\boldsymbol{r}-\boldsymbol{r}')P_A(\boldsymbol{r})P_C(\boldsymbol{r}')]+k_BT\cdot\\ &\sum_{\boldsymbol{r}}[P_A(\boldsymbol{r})\ln(P_A(\boldsymbol{r}))+P_B(\boldsymbol{r})\ln(P_B(\boldsymbol{r}))+P_C(\boldsymbol{r})\ln(P_C(\boldsymbol{r}))]\end{aligned} \tag{3}$$

where $V_{\alpha\beta}(\boldsymbol{r}-\boldsymbol{r}')$ is the interaction energy between α and β. The microscopic phase-field kinetic model for the ternary alloy is obtained through substituting Eqn.(3) into Eqn.(2).

3 Simulation results and analysis

3.1 Atomic morphologies evolution of γ' phase

Fig.1 shows atomic morphologies evolution of γ' phase for $NiAl_9Fe_6$ alloy. The matrix is in disordered state before 4 400 time steps. At that moment 2 or 3 faint γ' particles appear in the γ disordered matrix (Fig.1(a)). The number of the γ' phase increases with the time increasing, and these γ' sphere and ellipsoid particles independent with each other, are randomly distributed in disordered matrix. Then, the γ' ordered phases in the size quickly become big, while its number increases very slowly (Figs.1(b) and (c)). Since the atomic occupation probability becomes higher, the ordering degree of γ' phase continuously increases, the transformation of alloy system is gradually completed from the disordered phase to the ordered phase, and the two-phase common zone (γ and γ' phases) is formed (Fig.1(d)). So it is initially concluded that the precipitated γ' phase obeys the nucleation and growth mechanism during phase transformation. Finally, the formed γ' phase is a complex single-phase.

Now the ordering process of γ' phase will be clarified by analyzing in detail the concentration, l.r.o. parameter and the site occupation rules of the different atoms in γ' phase and order-disorder interphase boundary for the $NiAl_9Fe_6$ alloy.

3.2 Ordering in γ' ordered phase

3.2.1 Evolution of l.r.o. parameter and concentration curves

Now the ordering process of γ' phase is investigated by the l.r.o. parameter and concentration curves in the ordered particles A (Fig.1). Figs.2(a) and (b) shows l.r.o. parameter and concentration curves of the Al atoms in γ'

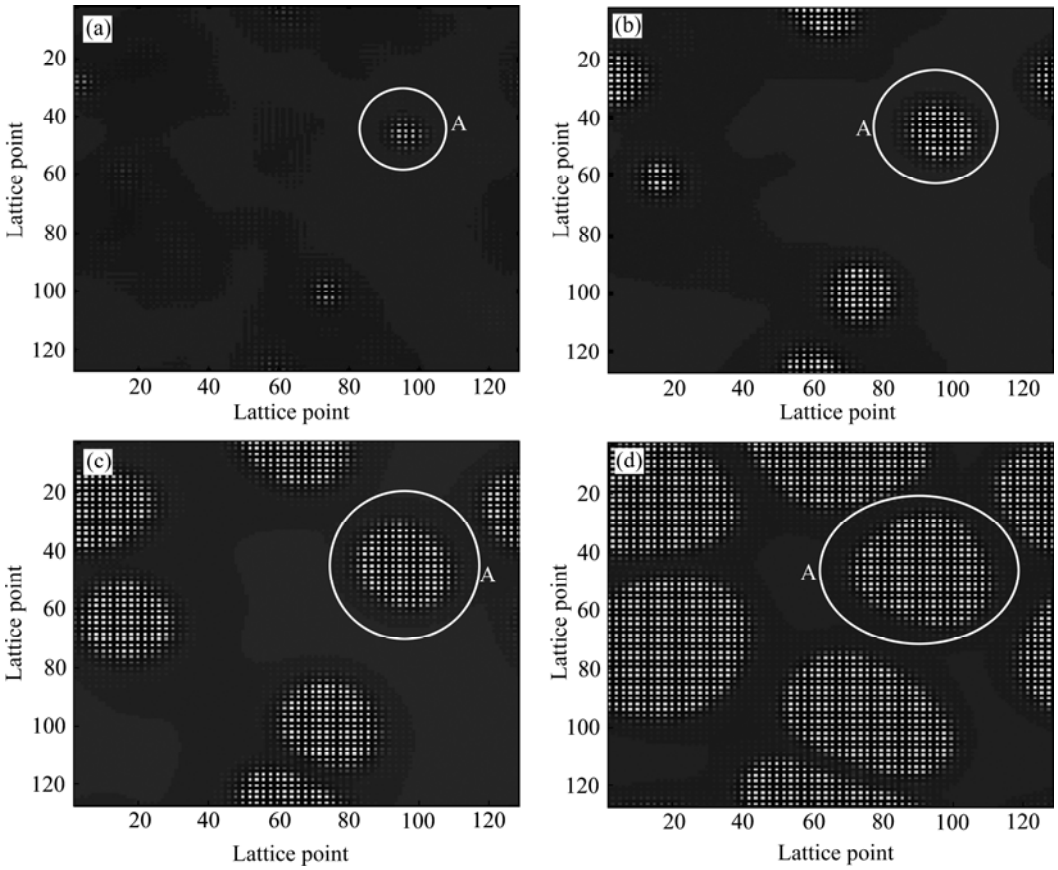

Fig.1 Atomic morphology evolutions of γ' phase for $NiAl_9Fe_6$ alloy at different time steps: (a) 4 400; (b) 7 000; (c) 12 000; (d) 50 000

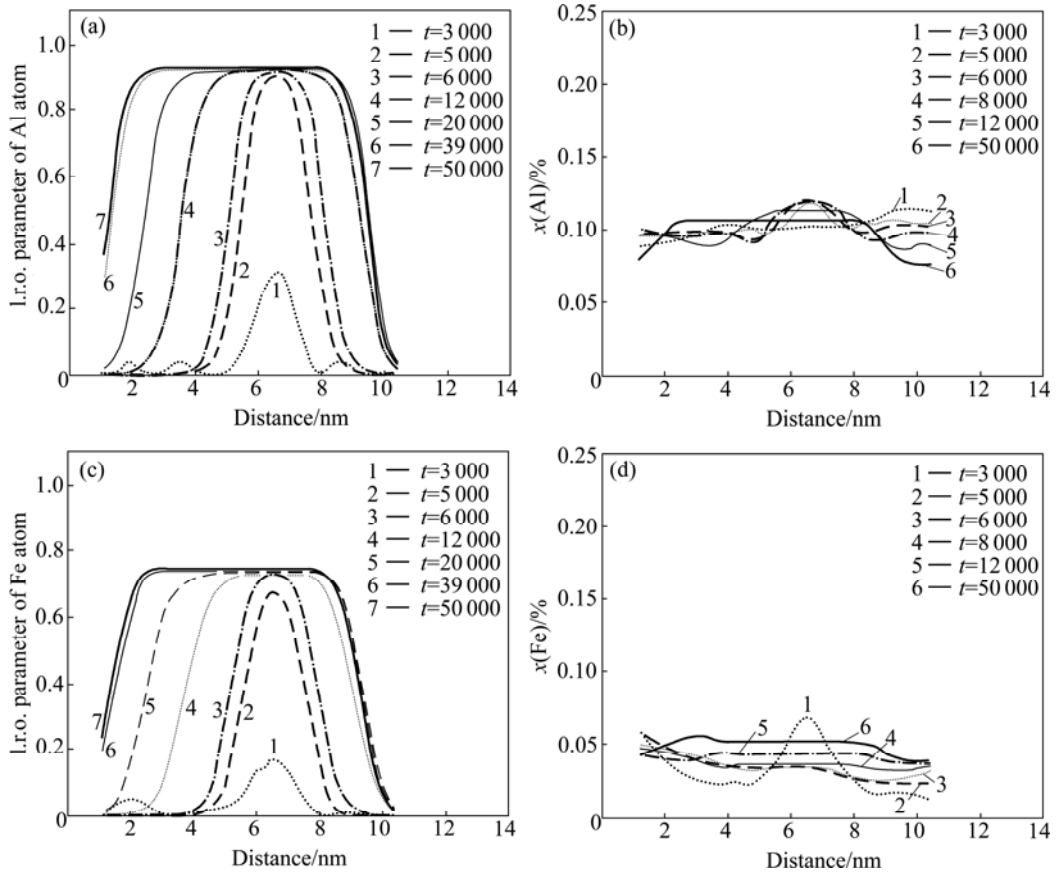

Fig.2 Curves of l.r.o. parameter and concentration in γ' phase at different time steps: (a) l.r.o. parameter of Al atom; (b) Concentration of Al atom; (c) l.r.o. parameter of Fe atom; (d) Concentration of Fe atom

phase at different aging time. Before 3 000 time steps, because the transformation from γ to γ' phase hasn't appeared, l.r.o. parameters have no change. The curves of l.r.o. parameter have obvious fluctuation in the center of nucleation with a particle appearing, while the concentration curves almost keep at certain level, which shows that the Al atomic clustering is later than its ordering progress. Then, l.r.o. parameter curves quickly rise, meanwhile, the corresponding concentration curves also slowly rise, which indicates that Al atoms occupy the β site to make the ordering degree increase. The values of two parameters reach their maximum until 6 000 time steps. And in subsequent process, l.r.o. parameter curves almost remain invariable in their height and broaden in their width, which corresponds to the growth and coarsening stage of γ' phase; yet, the concentration curves slowly fall and finally reach the equilibrium. It is concluded that Fe and Ni atoms begin to partly occupy β site during the precipitation process of the γ' phase, which results in the concentration of Al atoms falling down.

The l.r.o. parameter and concentration curves of Fe atoms are approximately similar to those of Al atoms (Figs.2(c) and (d)). The distinctions between them lie in: 1) the l.ro. parameter values of Fe atoms are lower than those of Al atoms, from which it is concluded that the ordering degree of Fe atoms is lower than that of Al atoms in the γ' phase; 2) the concentration curves of Fe atoms change from rising to quickly falling, and then slow rising; 3) the clustering of Fe atoms precedes the clustering of Al atoms.

From analysis above, the atomic clustering and ordering process of γ' phase during phase transformation can be clearly seen. In order to clarify the different site occupation of three atoms in $L1_2$ superstructure, we make the further explanation by the curves of the atomic site occupation in the γ' phase.

3.2.2 Evolution of atomic site occupation in γ' phase

From the evolution of atomic site occupation curves (Figs.3(a) and (b)), it can be seen that the α site is mainly occupied by Ni atoms, yet Al and Fe atomic occupation probabilities are almost zero at α site (Fig.3(a)). At the β site, the occupation probability of Al atoms quickly increases at the first moment and reaches the equilibrium value (about 0.45); Fe atoms gradually occupy the β site from 3500 time steps, and the occupation probability slowly increases and finally reaches the maximum (about 0.2); meanwhile, Ni atoms also occupy the β site, which is at the same time as the Al atoms, and the occupation probability reaches the maximum, henceforth its value slowly falls, and reaches the equilibrium of 0.36 (Fig.3(b)) (the Ni atoms have the antisite phenomenon, which was also reported in the Ref.[15]). Finally, the β site is occupied in common by the Al, Fe and Ni atoms, the equilibrium state is reached, and the $Ni_3(AlFeNi)$ structure of γ' phase is formed.

3.3 Ordering at γ'-γ interphase boundary

Fig.4 shows an enlarged figure about the course of atomic site occupation at γ'-γ interphase boundary, which clearly shows the process of the order-disorder phase transformation. In this simulation, the rectangular zone of Figs.4(a)−(d) is chosen to investigate the atomic ordering and site occupation from the γ' to the γ interphase boundary.

3.3.1 Long-range ordering progress of different atoms at γ'-γ interphase boundary

Figs.5(a) and (b) show the l.r.o. curves of Al and Fe atoms at γ'-γ interphase boundary, which shows that the long-range ordering degree of Al atoms is obviously higher than that of Fe atoms. The values of l.r.o. parameters of Al and Fe atoms gradually rise on the whole, which corresponds to the gradual increase of the Al and Fe atomic ordering degree and the growth of the ordered particles. After the 10 000 time steps the l.r.o. parameters almost have no change, the order-disorder transformation is basically completed, and the equilibrium state is finally reached at interphase boundary.

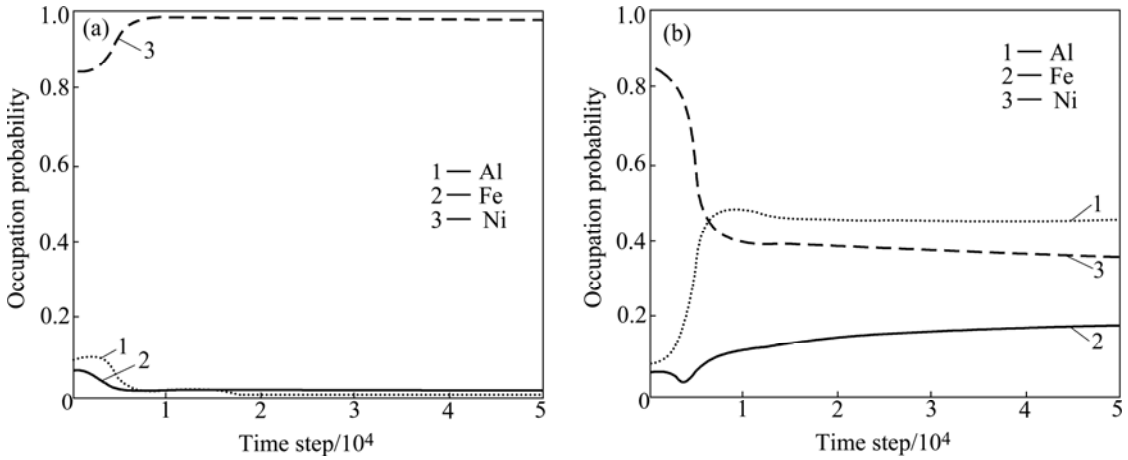

Fig.3 Evolutions of different atomic site occupation in $NiAl_9Fe_6$ alloy: (a) α site; (b) β site

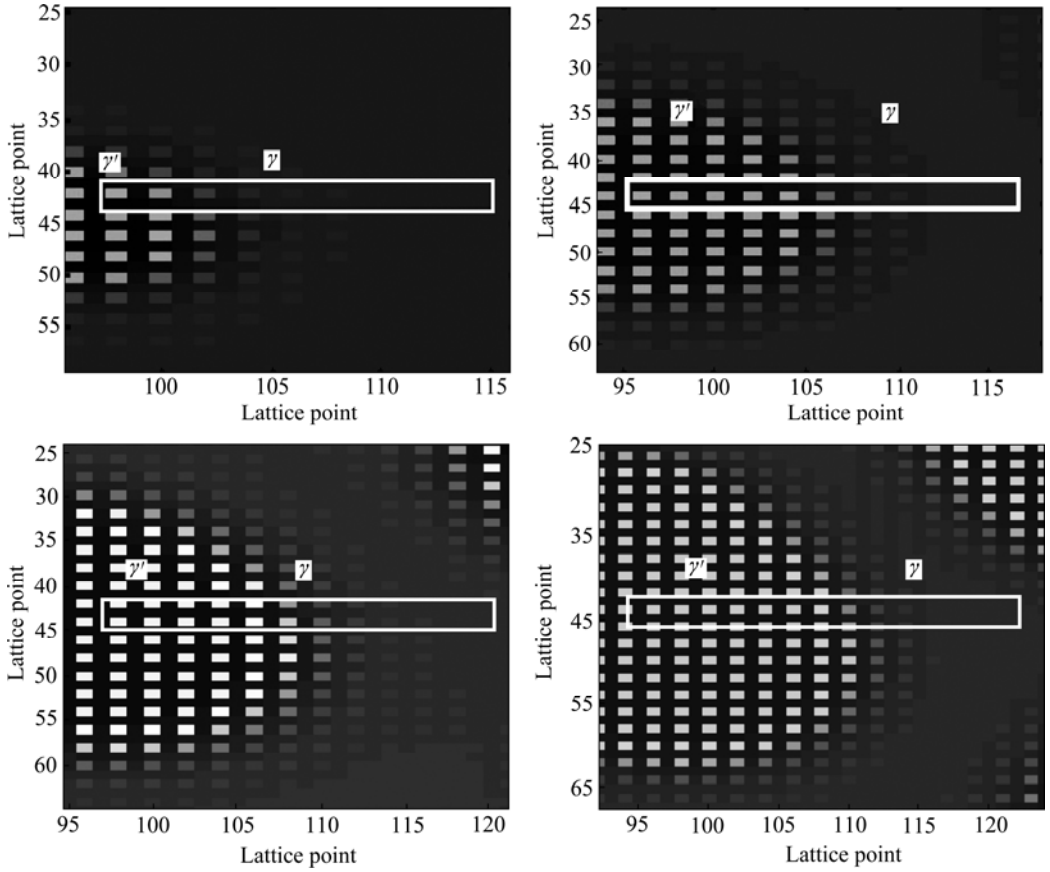

Fig.4 Enlarged figures of atomic site occupation at γ'-γ interphase boundary in $NiAl_9Fe_6$ alloy at different time steps: (a) 5 000; (b) 8 000; (c) 12 000; (d) 50 000

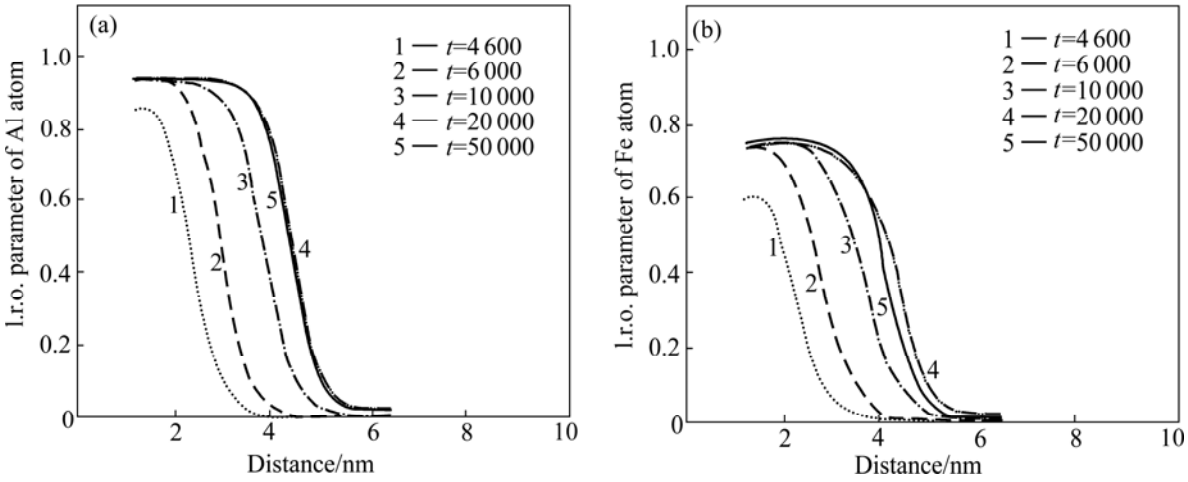

Fig.5 l.r.o. curves at order-disorder interphase boundary at different time steps: (a) Al atom; (b) Fe atom

Meanwhile, it is found that the order-disorder interphase boundary, which is in a gradually transitional state, has certain width (about 2 nm). Thus the result denies the conclusion of classical theory that the order-disorder phase boundary has the sharp interface.

3.3.2 Evolution rules of atomic site occupation at γ'-γ interphase boundary

Fig.6 shows the evolving curves of atomic site occupation at β site at γ'-γ interphase boundary (the lattice of the rectangular zone in Fig.4). In the zone 1 (γ' phase zone), Fe atomic site occupation shows the slowly increasing trend from the lower value since the 5 000 time steps, and the value of the atomic site occupation increases at the higher speed near the zone 2 (transitional zone). Finally, the values of atomic occupation reach the uniformity at the different lattice site (about 0.2) in the zone 1; the trend of Fe atomic site occupation in the zone 2 is similar to that in the zone 1 on the whole, but its value

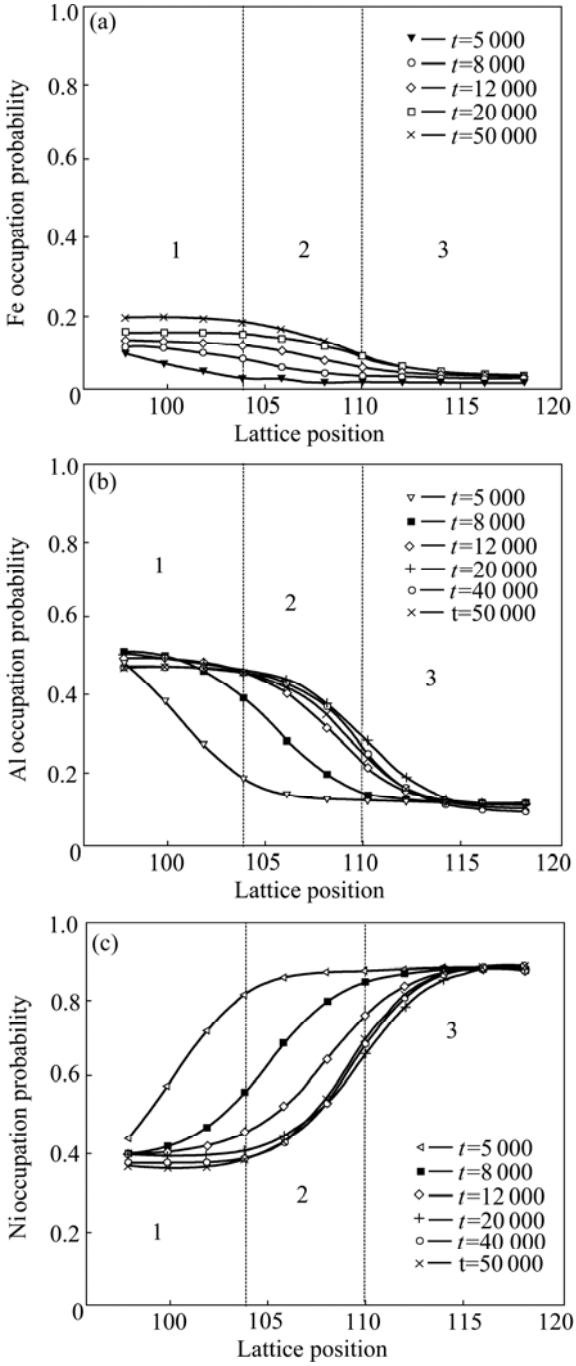

Fig.6 Evolutions of atomic site occupation at β site of γ'-γ interphase boundary: (a) Fe atom; (b) Al atom; (c) Ni atom

of site occupation is relatively lower at the different sites and slowly falls from zone 2 to 3 (γ phase zone); the value of Fe atomic site occupation is much lower and almost keeps the constant 0.04 in the zone 3 (Fig.6(a)). The site occupation curves of Al atoms are basically similar to those of Fe atoms. However, the value of site occupation is higher than that of Fe atoms and it almost has no change after 12 000 time steps. Al atomic occupation is very quick at the β site in zone 1 and 2 (Fig.6(b)), which shows that Al atomic ordering process is more quickly than Fe atoms at the interphase boundary during the formation of the ordered phase, which is consistent with the result of l.r.o parameter curves. Whereas, the rule of Ni atomic site occupation which gradually rises from zone γ' to γ phase zone is completely opposite to that of Al and Fe atoms (Fig.6(c)). The results above show that three atoms gradually occupy the corresponding lattice site by the diffusion and atomic migration, and then complete the order-disorder transformation.

Using the atom probe methods, ALMAZOUZI et al[9] thought that Fe atoms preferentially substitute Al atoms and occupy the β site at low Fe concentration. JIANG et al[15] find that in Ni-rich Ni_3Al, the Fe atoms show a preference for the Al site with the increasing temperature; in binary Ni_3Al alloy exists Ni antisites in Ni-rich Ni_3Al. The results that Fe atoms mostly occupy the β site and the Ni atoms appear at the β site (antisite behaviour) well agree with the experimental and theoretic results above.

3.3.3 Volume evolution of ordered and disordered phase

Fig.7(a) shows the evolution of the volume fraction

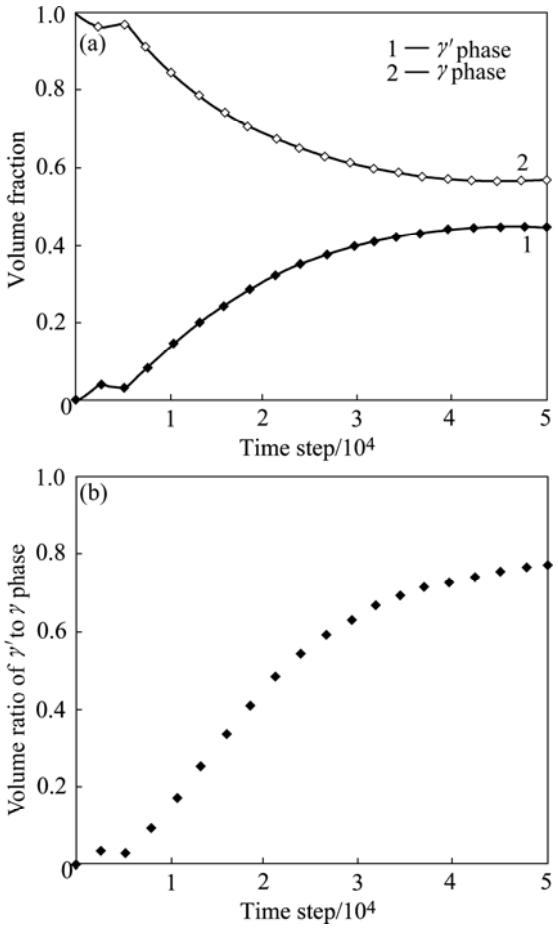

Fig.7 Evolution of volume fraction curves in $NiAl_9Fe_6$ alloy: (a) γ' and γ phase volume fraction; (b) Volume ratio of γ' to γ phase

of γ' and γ phase. The γ' phase appears a little at the early aging stage and obviously increases in number with the aging proceeding, while the number of the corresponding γ phase decreases. At the later aging stage the phase transformation becomes slower, and the volume of the γ' phase almost has no change, which finally comes to 41% of the total volume. From the ratio of γ' phase to γ phase (Fig.7(b)), it can be seen that the order-disorder transformation is very quick, and the volume ratio is almost linearly proportional to the time t before the 30 000 time steps, while at the latter stage the volume of γ' phase increases slowly. Correspondingly it is shown that the nucleation and the growth of ordered phase are mainly at the early aging stage, while the latter stage is mainly coarsening. In two-phase common zone formed for $NiAl_9Fe_6$ alloy, the volume of γ' phase is less than that of γ phase, and the volume ratio of ordered to disordered phase is about 77%.

4 Conclusions

1) The formed γ' phase is a complex structure of Ni_3(AlFeNi) single-phase, and the precipitation of γ' phase obeys the non-classical nucleation and growth mechanism during the γ(fcc) → γ(fcc)+$\gamma'(L1_2)$ phase transformation for $NiAl_9Fe_6$ alloy.

2) In the γ' phase, the ordering degree of the Al atoms is obviously higher than that of the Fe atoms, and the Al atomic clustering is later than its ordering process, while the case of Fe atoms is opposite. The Al atomic concentration changes from falling to rising, and then falling, while the Fe atomic concentration changes from rising to falling to slowly rising. The α site is occupied by Ni atoms; at the β site, the Fe atoms substitute for the part of Al atoms, and their site occupation probabilities are obviously lower than those of Al atoms. Meanwhile, Ni atoms also occupy the β site, and finally the site occupation probability reaches 0.36. In a word, the β site is occupied in common by Al, Fe and Ni atoms.

3) At the γ'-γ interphase boundary, the long-range ordering degree of Al atoms is higher than that of Fe atoms. From γ' to γ interphase boundary, the site occupation probabilities of the Fe atoms vary from high to the low at the β site. The case of the Al atoms is similar to Fe atoms, but their values are obviously higher than those of Fe atoms. The rule of Ni atomic site occupation is opposite to both Al and Fe atoms.

4) The volume of γ' phase is less than that of the γ phase in the formed two-phase zone of ordering transformation in $NiAl_9Fe_6$ alloy, and finally the volume ratio of ordered to disordered phase is about 77%.

References

[1] CHANTAL K S, KEVIN E Y, RONALD D N, DAVID N S. Temporal evolution of the nanostructure and phase compositions in a model Ni-Al-Cr alloy [J]. Acta Mater, 2006, 54(12): 3199−3210.

[2] CAHN R W, SIEMERS P A, GEIGER J E, BARDHAN P. The order-disorder transformation in Ni_3Al and Ni_3Al-Fe alloys (I): Determination of the transition temperatures and their relation to ductility [J]. Acta Metall, 1987, 35(11): 2737−2751.

[3] LI Yong-sheng, CHEN Zheng, WANG Yong-xin, LU Yan-li. Computer simulation of γ' and θ phase precipitation of Ni-Al-V alloy using microscopic phase-field method [J]. Trans Nonferrous Met Soc China, 2005, 15(1): 57−63.

[4] LECHERMANN F, FÄHNLE M, SANCHEZ J M. First-principles investigation of the Ni-Fe-Al system [J]. Intermetallics, 2005, 13(10): 1096−1109.

[5] CHU Z, CHEN Z, WANG Y X, LU Yan-li, LI Yong-sheng. Atomic-scale computer simulation for ternary alloy Ni-Cr-Al during early precipitation process [J]. Progress in Natural Science, 2005, 15(7): 656−660.

[6] CHU Zhong, CHEN Zheng, WANG Yong-xin, LU Yan-li , ZHANG Jian-jun. Microscopic phase-field simulation of atom substitution behaviour in Ni-Cr-Al alloy [J]. Chinese Phys Lett, 2005, 22(8): 1841−1844.

[7] CHANTAL K S, RONALD D N, DAVID N S. Compositional pathways and capillary effects during isothermal precipitation in a nondilute Ni-Al-Cr alloy [J]. Acta Mater, 2007, 55(7): 119−130.

[8] KOZUBSKI R, SOLTYS J. Long-range ordering kinetics and ordering energy in Ni_3Al-based γ' alloys [J]. Intermetallics, 1993, 1(3): 139−150.

[9] ALMAZOUZI A, NUMAKURA H, KOIWA M, HONO K, SAKURAI T. Site occupation preference of Fe in Ni_3Al: An atom-probe study [J]. Intermetallics, 1997, 5(1): 37−43.

[10] ANNIE B, SANTHOSHINIB D, KAUL S N. Site occupancy of Fe in ternary $Ni_{75-x}Fe_{x+y}Al_{25-y}$ alloys [J]. Pramana Journal of Physics, 2003, 60(3): 517−520.

[11] JIANG C, GLEESON B. Site preference of transition metal elements in Ni_3Al [J]. Scripta Materialia, 2006, 55(5): 433−436.

[12] KHACHATUYRAN A G. Theory of structural transformations in solids [M]. New Tork: Wiley, 1983: 321−323.

[13] PODURI R, CHEN L Q. Computer simulation of atomic ordering and compositional clustering in the pseudobinary Ni_3Al-Ni_3V system [J]. Acta Mater, 1998, 46(5): 1719−1729.

[14] CHEN L Q. Computer simulation of spinodal decomposition in ternary systems [J]. Acta Metal Mater, 1994, 42(10): 3503−3513.

[15] JIANG C, SORDELET D J, GLEESON B. Site preference of ternary alloying elements in Ni_3Al: A first-principles study [J]. Acta Mater, 2006, 54(4): 1147−1154.

(Edited by LI Xiang-qun)